

# Cross Sections for Electron Collisions with NF<sub>3</sub>

Mi-Young Song<sup>a)</sup>,<sup>1</sup> Jung-Sik Yoon,<sup>1</sup> Hyuck Cho,<sup>2</sup> Grzegorz P. Karwasz,<sup>3</sup> Viatcheslav Kokoouline,<sup>4</sup> Yoshiharu Nakamura,<sup>5</sup> James R. Hamilton,<sup>6</sup> and Jonathan Tennyson<sup>6</sup>

<sup>1)</sup> Plasma Technology Research Center, National Fusion Research Institute, 814-2, Osikdo-dong, Gunsan, Jeollabuk-do, 573-540, South Korea<sup>a)</sup>

<sup>2)</sup> Department of Physics, Chungnam National University, Daejeon 305-764, South Korea

<sup>3)</sup> Faculty of Physics, Astronomy and Applied Informatics, University Nicolaus Copernicus, Grudziadzka 5, 87-100, Toruń, Poland

<sup>4)</sup> Department of Physics, University of Central Florida, Orlando, FL 32816, USA

<sup>5)</sup> 6-1-5-201 Miyazaki, Miyamae, Kawasaki, 216-0033, Japan

<sup>6)</sup> Department of Physics and Astronomy, University College London, Gower Street, London WC1E 6BT, UK

(Revised 24 January 2022)

Cross section data are compiled from the literature for electron collisions with nitrogen trifluoride (NF<sub>3</sub>) molecules. Cross sections are collected and reviewed for total scattering, elastic scattering, momentum transfer, excitations of rotational and vibrational states, dissociation, ionization, and dissociative attachment. For each of these processes, the recommended values of the cross sections are presented. The literature has been surveyed up to the end of 2016.

PACS numbers: 34.80.Bm, 52.20.Fs

Keywords: electron collisions, total cross sections, ionization, dissociation, attachment, evaluation

## I. INTRODUCTION

Nitrogen trifluoride or trifluoramine (NF<sub>3</sub>) gas is widely used in plasma processing technology. NF<sub>3</sub> is used in a number of plasma processes where it is often used as a source of F atoms due to ease of production these atoms via dissociative electron attachment (DEA) and electron impact dissociation both from NF<sub>3</sub> itself and from NF<sub>2</sub> and NF fragment species. The exothermicity from these dissociative processes also provides an important gas heating mechanism. Use of NF<sub>3</sub> in plasma etching, particularly in mixtures with O<sub>2</sub>, see Ref.<sup>1</sup>, provides a source of F<sup>-</sup> ions due to enhanced dissociative electron attachment process at low (about 1 eV) energies. NF<sub>3</sub> is widely used for semiconductor fabrication processes which include direct etching<sup>2,3</sup>, reactor cleaning<sup>4</sup> and remote plasma sources<sup>5</sup>, where use of pure NF<sub>3</sub> typically limits the reactants reaching the processing chamber to F<sub>x</sub> and NF<sub>x</sub> species only. NF<sub>3</sub> is also used in the production of thin films<sup>6,7</sup> and solar cells<sup>8,9</sup>; it provides the initial gas for the HF chemical laser<sup>10-12</sup>. NF<sub>3</sub> is actually a greenhouse gas with a very high global warming potential which has led to concern on how it is used in the various technologies discussed above<sup>13</sup>. In spite of its importance, experimental studies of electron scattering on NF<sub>3</sub> are rather sparse: for total<sup>14</sup> and elastic<sup>15</sup> cross section measurements come from single laboratories, more measurements exist for ionization<sup>16-18</sup> and dissociative electron attachment<sup>19-21</sup>. In absence of experiments, several calculations<sup>22-25</sup> have been performed. Some reference cross sections based both on experiments

and calculations were reported by Lisovskiy *et al.*<sup>26</sup> in modeling electron transport coefficients and by Huang *et al.*<sup>1</sup> for modeling remote plasma sources in NF<sub>3</sub> mixtures. Here we perform a detailed analysis of available data for electron scattering on NF<sub>3</sub>, to yield recommended total, elastic, momentum transfer, ionization, dissociation into neutrals, and vibrational, rotational, and electronic excitation cross sections. In the ground electronic state <sup>1</sup>A' the molecule has a shape of a pyramid of the C<sub>3v</sub> group with fluorine atoms forming an equilateral triangle. Due to its symmetry, the dipole moment of the molecule is aligned along the C<sub>3</sub> symmetry axis. Geometry, electric dipole moment, and rotational constants are specified in Table I.

TABLE I. Properties of NF<sub>3</sub> at the equilibrium position of the ground electric state. *A*, *B*, and *C* are rotational constants;  $\alpha_0$  is the spherical dipole polarizability.

Property	Value
F-N bond length <sup>27</sup>	1.365 Å
FNF angle <sup>27</sup>	102.4°
Dipole moment <sup>27</sup>	0.235 D
<i>A</i> = <i>B</i> <sup>28</sup>	10.6810819(15) GHz
<i>C</i> <sup>28</sup>	5.8440 GHz
$\alpha_0$ <sup>29</sup>	$3.62 \times 10^{-30}$ m <sup>3</sup>

## II. TOTAL SCATTERING CROSS SECTION

Practically, absolute data by Szmytkowski *et al.*<sup>14</sup> at 0.5-370 eV collision energy is the only measurement of total cross section in NF<sub>3</sub>. The beam attenuation deBeer-Lambert's method was used, with a 3 cm long scattering

<sup>a)</sup> Electronic mail: corresponding author at mysong@nfri.re.kr

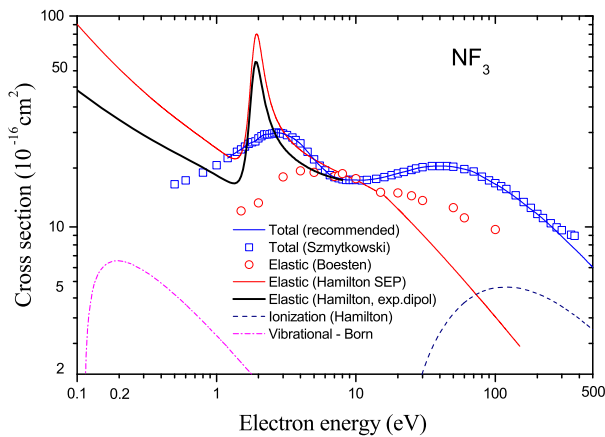


FIG. 1. Total cross sections by Szymtkowski *et al.*<sup>14</sup> compared to experimental integral elastic cross sections of Boesten *et al.*<sup>15</sup>, integral vibrational excitation (Born approximation for the  $\nu_3$  IR active mode) and total ionization (theory by Rahman *et al.*<sup>18</sup>).

cell and  $2 \times 10^{-3}$  sr mean angular resolution. Systematic errors declared (gas outflow from scattering cell, determination of the scattering length, current non-linearity, pressure and temperature measurements) are within 5%, out of which the declared angular resolution error is 0.2% at low energies, rising to 1% at 100 eV and 2-3% in the high energy limit. The statistical spread (one standard deviation of their weighted mean values) is 1.5% below 1 eV and below 1% at intermediate energies. Total cross sections<sup>14</sup> are compared to experimental elastic<sup>15</sup>, ionization<sup>18</sup> and vibrational excitation (calculated in Born approximation) in Fig. 1.

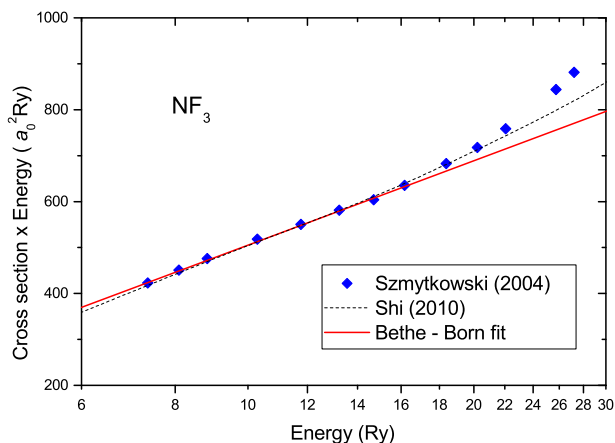


FIG. 2. Bethe-Born plot of total cross sections by Szymtkowski *et al.*<sup>14</sup> in their high energy limit. Total cross sections from modified additivity rule of Shi *et al.*<sup>30</sup> are also shown for comparison (data read from their fig. 1).

Calculations of integral elastic cross section<sup>24,25</sup> predict a resonant structure which is much narrower (and higher) than the resonance seen in the total cross

section<sup>14</sup>, see Fig. 1. This may be due to the neglect of nuclear motion in the calculations. Similar discrepancies between theory and experiments are observable for molecular targets, like CO<sub>2</sub>, N<sub>2</sub>O: in these molecules the vibrational excitation constitutes a significant part (about 1/3) of the total cross section<sup>31</sup>. Calculations for N<sub>2</sub>O<sup>32</sup>, similar to those for NF<sub>3</sub>, also give resonant maxima higher than the experiment. Note also that NF<sub>3</sub> is a polar molecule, so the interaction with the incoming electron is more attractive in comparison to targets like CH<sub>4</sub>, and this shifts maxima to lower energies. Two recent calculations<sup>24,25</sup> indicate that the total cross section should rise in the limit of zero energy, due to the polar character of the molecule. Unfortunately, this was not observed in the experiment<sup>14</sup>, probably because the measurements were stopped at energies higher than the range of such a rise. The rather poor angular resolution of Szymtkowski *et al.*'s apparatus make their measurement vulnerable to the angular resolution error at high energies. To verify this, in Fig. 2 we show a Bethe-Born plot of total cross sections, as done in our previous review in CH<sub>4</sub><sup>33</sup>,

$$\sigma(E) = A/E + B \log(E)/E, \quad (1)$$

where energy is expressed in Rydbergs, Ry = 13.6 eV and the cross sections is expressed in atomic units  $a_0^2 = 0.28 \times 10^{-16} \text{cm}^2$ . Parameters of the fit, based on experimental points<sup>14</sup> between 100-220 eV are  $A = -110 \pm 10$  and  $B = 610 \pm 20$ . Contrary to expectations, the plot in Fig. 2 suggests that total cross sections given by Szymtkowski *et al.*<sup>14</sup> are overestimates in their high energy limit. We note however that Bethe-Born analysis is not fully justified at energies of few hundreds of eV, see discussion in Ref.<sup>34,35</sup>. Therefore, in Fig. 2 we plot also total cross sections obtained by the additivity rule<sup>30</sup>: these data coincide with the present Bethe-Born fit up to 200 eV and then deviate slightly upwards. Unfortunately, no information on uncertainties was given by Shi *et al.*<sup>30</sup>. Table II gives our recommended total cross sections which are based on the experiment of Ref.<sup>14</sup> at energies 1-90 eV and on the Bethe-Born fit at higher energies.

### III. ELASTIC SCATTERING CROSS SECTION

Available data for elastic electron scattering from NF<sub>3</sub> are very sparse. The first theoretical study on low-energy electron collision processes in NF<sub>3</sub> was reported by Rescigno<sup>22</sup> which included Kohn variation calculations of elastic differential cross sections (DCS) and integral cross sections (ICS) for electrons with energies in the range 0–10 eV. The only comprehensive experimental study, which reported elastic DCS, ICS, and momentum transfer cross sections (MTCS) for energies between 1.5 and 100 eV and for angles between 15° (20° for energies below 8 eV) and 130°, was published by Boesten *et al.*<sup>15</sup> Subsequently, a Schwinger multichannel theoretical approach<sup>23</sup> reported corresponding cross sections for

TABLE II. Recommended total cross sections (TCS), in  $10^{-16}$   $\text{cm}^2$  units. In the region 1-100 eV recommended values are adopted from the experiment by Szmytkowski *et al.*<sup>14</sup>. Values at 100-500 eV are obtained from parameters of the Bethe-Born plot, Fig. 2. The overall uncertainty of TCS is  $\pm 10\%$  at 1-100 eV and 15% above 100 eV. Additionally from the  $\pm 10\%$  uncertainty, TCSs below 1 eV<sup>14</sup> may be underestimated due to an angular resolution error, by the amount rising with lowering energy. The energy determination is  $\pm 0.1\text{eV}$ .

Electron energy	TCS	Electron energy	TCS	Electron energy	TCS
0.5	15.9	3.7	25.8	35	19.4
0.6	16.6	4.0	24.9	40	19.4
0.8	18.1	4.5	22.7	45	19.4
1.0	19.6	5.0	20.9	50	19.3
1.2	21.2	5.5	19.5	60	18.8
1.4	22.7	6.0	18.5	70	18.3
1.5	23.3	6.5	17.6	80	17.3
1.6	24.0	7.0	17.2	90	16.6
1.7	24.8	7.5	17.0	100	15.9
1.8	25.2	8.0	16.8	110	15.4
1.9	25.4	8.5	16.7	120	14.8
2.0	26.3	9.0	16.7	140	13.8
2.1	26.9	9.5	16.7	160	12.9
2.2	27.4	10	16.7	180	12.1
2.3	27.5	11	16.6	200	11.5
2.4	27.5	12	16.7	220	10.9
2.5	27.7	14	16.9	250	10.1
2.6	27.8	16	17.2	275	9.51
2.7	28.0	18	17.6	300	9.00
2.8	27.9	20	17.9	350	8.16
2.9	27.8	22	18.2	400	7.48
3.0	27.7	25	18.6	450	6.91
3.2	27.2	27	18.9	500	6.43
3.5	26.5	30	19.2		

electron energies in the range 0–60 eV. Complete numerical values of Boesten *et al.*<sup>15</sup> and 4 representative figures for DCS's are presented in Table III and Fig. 3. Their ICS's are also given in Table III and Fig. 4. Theoretical ICS's of Joucoski and Bettega<sup>23</sup> and the total cross sections of Szmytkowski *et al.*<sup>14</sup> are plotted on the Fig. 4 for comparison. Generally a good agreement is found between the results from the calculation by Joucoski and Bettega and the experiment by Boesten *et al.*, except a few points between 5 eV and 10 eV, where the theory exceeds the total cross sections of Szmytkowski *et al.* The permanent dipole moments of  $\text{NF}_3$  is 0.0944 au, which is small compared to other polar molecules such as  $\text{NH}_3$  (0.578 au) and  $\text{H}_2\text{O}$  (0.728 au). Therefore, dipole interaction between the electron and  $\text{NF}_3$  would not be important in this collision system<sup>15</sup>. And, dipole-enhanced forward scattering is restricted to small angles, usually below 10–20°, and Boesten *et al.* claimed that this was confirmed in the calculations of Rescigno<sup>22</sup> whose DCS at 20° reflect their own data. In the energy and angular ranges of the experiments by Boesten *et al.*, there is no evidence that their results are unreasonably underestimated, even though there could still be a few pos-

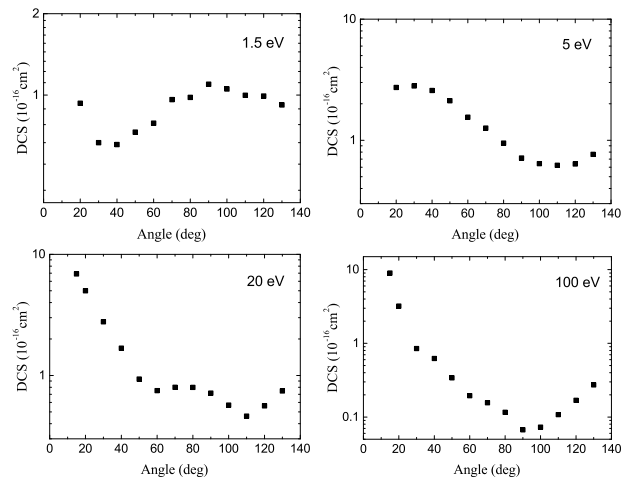


FIG. 3. Recommended elastic DCS for four representative energies<sup>15</sup>.

sibilities of slight over- or under-estimation which may not be included in their uncertainty estimation. So our recommended data is consequently taken from the measurements of Boesten *et al.* Similarly, we recommend their ICS's. Boesten *et al.* estimated the uncertainties of DCS as 15 % and of ICS as 30-50 %. They estimated the contributions of the low and high angle extrapolations separately, and we present these in their original forms at the bottom of Table III. The contributions of the low and high angle extrapolations are indicated as L% and R%, respectively. Very recently, Hamilton *et al.* published calculated ICS's<sup>25</sup> and are presented in Fig.4 for comparison.

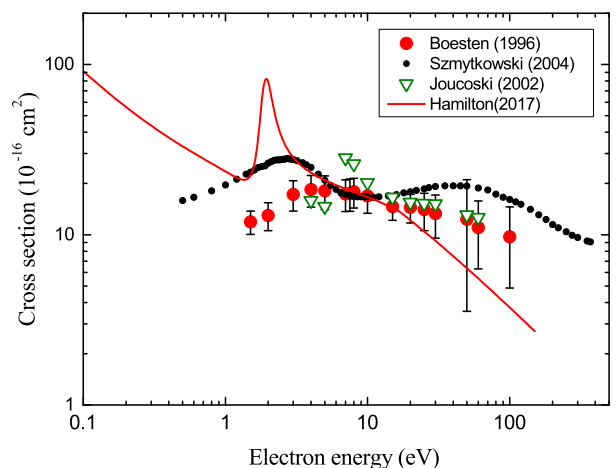


FIG. 4. Recommended elastic integral cross sections with the selected sets of data from the publications<sup>14,15,23,25</sup>.

TABLE III. Recommended elastic electron scattering cross sections from NF<sub>3</sub>. DCS's are in the units of  $10^{-16} \text{ cm}^2\text{sr}^{-1}$ . Recommended elastic integral cross sections are also given at the bottom in the units of  $10^{-16} \text{ cm}^2$  [Ref. 15]. The uncertainties of DCS are 15 % and of ICS are 30-50 %.

Angle (deg)	1.5eV	2eV	3eV	4eV	5eV	7eV	7.5eV	8eV	10eV	15eV	20eV	25eV	30eV	50eV	60eV	100eV
	DCS	DCS	DCS	DCS	DCS	DCS	DCS	DCS	DCS	DCS	DCS	DCS	DCS	DCS	DCS	DCS
15	—	—	—	—	—	—	—	—	3.323	4.641	6.890	9.051	10.710	12.330	11.200	9.000
20	0.933	1.430	2.199	2.960	2.729	2.671	2.896	2.908	3.168	3.946	5.006	6.490	6.946	6.715	5.955	3.201
30	0.667	1.216	2.436	2.949	2.807	2.932	3.036	3.132	3.037	3.077	2.777	2.863	2.657	1.838	1.243	0.851
40	0.656	1.078	2.331	2.822	2.577	2.868	2.731	2.699	2.680	2.107	1.680	1.358	1.004	0.666	0.671	0.623
50	0.729	1.197	2.052	2.511	2.119	2.123	2.224	2.115	1.934	1.271	0.934	0.742	0.616	0.621	0.537	0.340
60	0.787	1.152	1.768	1.818	1.552	1.655	1.517	1.460	1.390	0.826	0.750	0.688	0.639	0.601	0.328	0.195
70	0.962	1.074	1.329	1.297	1.261	1.137	1.108	1.209	0.954	0.715	0.799	0.747	0.671	0.340	0.232	0.156
80	0.981	1.100	1.114	1.099	0.947	0.808	0.851	0.868	0.737	0.725	0.798	0.665	0.509	0.196	0.155	0.116
90	1.097	1.011	0.920	0.794	0.714	0.727	0.719	0.766	0.702	0.786	0.715	0.510	0.320	0.116	0.109	0.067
100	1.053	0.884	0.685	0.640	0.641	0.663	0.704	0.702	0.694	0.738	0.569	0.322	0.191	0.093	0.093	0.073
110	0.998	0.843	0.598	0.542	0.622	0.666	0.704	0.707	0.673	0.610	0.462	0.295	0.200	0.146	0.152	0.108
120	0.992	0.778	0.584	0.539	0.637	0.652	0.661	0.639	0.626	0.555	0.561	0.440	0.376	0.314	0.265	0.169
130	0.920	0.723	0.576	0.604	0.765	0.655	0.645	0.623	0.605	0.598	0.746	0.725	0.623	0.483	0.378	0.273
ICS	11.90	12.98	17.24	18.41	18.11	17.35	17.47	17.89	16.91	14.60	14.48	14.05	13.33	12.32	11.03	9.72
L%	4	5	7	7	8	7	8	13	6	9	13	18	24	35	41	47
R%	15	18	19	20	21	20	20	15	20	14	14	17	15	62	13	17

#### IV. MOMENTUM TRANSFER CROSS SECTION

The momentum-transfer cross section for electron-NF<sub>3</sub> collisions was determined in the same studies, mentioned above<sup>15,22,23,25</sup>, where the elastic cross sections were measured or computed. The experimental data by Boesten *et al.*<sup>15</sup> is not complete, especially, at energies below 1 eV. Out of the three theoretical studies<sup>22,23,25</sup>, the most recent one by Hamilton *et al.*<sup>25</sup> appears to be the most accurate one due to a more accurate method (complete active space-configuration interaction) and a larger basis set employed. However, the position of the resonance near 1 eV in this study is shifted towards lower energies compared to the experimental data. The width of the resonance in all theoretical studies is significantly narrower than in the experiment. Therefore, at energies above 1 eV, where experimental data exist, we recommend the experimental data, namely, the one by Boesten *et al.*<sup>15</sup> and energies below 1 eV, the theoretical results by Hamilton *et al.*<sup>25</sup>. The available theoretical and experimental data as well as the recommended set, are shown in Fig. 5. The values of the recommended data given in Table IV. Lisovskiy *et al.*<sup>26</sup> measured the drift velocity of electrons in NF<sub>3</sub> in a limited range of high reduced electric field  $E/p$  and compared their measurements with the results of the BOLSIG+ calculations using the momentum transfer cross sections of Boesten *et al.*<sup>15</sup>, and Joucoski and Bettega<sup>23</sup>. Agreement was satisfactorily, especially with calculation using the latter momentum transfer cross section.

#### V. ROTATIONAL EXCITATION CROSS SECTION

Due to its  $C_{3v}$  symmetry at equilibrium geometry, NF<sub>3</sub> is a symmetric top in the rigid-rotor approximation. It is an oblate rotor with rotational constants given in Table I. As for other symmetric top molecules, the rotational levels of NF<sub>3</sub> are characterized by two quantum numbers,

TABLE IV. The recommended momentum-transfer cross-section. The data below 0.65 eV are from Hamilton *et al.*<sup>25</sup> and above 1.5 eV is from Boesten *et al.*<sup>15</sup>. Energies are in eV, the cross sections are in units of  $10^{-16} \text{ cm}^{-1}$ .

Electron Energy	MTCS	Electron Energy	MTCS	Electron Energy	MTCS
6.74E-3	128.5	0.188	19.50	4.78	14.97
7.43E-3	117.6	0.208	19.15	5.27	14.83
8.20E-3	107.7	0.229	18.82	5.82	14.63
9.04E-3	98.80	0.253	18.52	6.41	14.42
9.97E-3	90.72	0.279	18.23	7.07	14.22
0.0110	83.41	0.308	17.95	7.80	13.30
0.0121	76.80	0.339	17.68	8.61	12.91
0.0134	70.83	0.374	17.42	9.49	13.57
0.0148	65.43	0.413	17.16	10.47	13.20
0.0163	60.56	0.455	16.91	11.55	12.34
0.0179	56.16	0.502	16.65	12.74	11.45
0.0198	52.19	0.554	16.35	14.05	10.73
0.0218	48.61	0.611	15.99	15.49	10.32
0.0241	45.38	0.674	15.60	17.09	10.24
0.0266	42.47	0.743	15.17	18.85	10.13
0.0293	39.85	0.820	14.74	20.79	9.63
0.0323	37.49	0.904	14.31	22.93	9.03
0.0356	35.36	1.00	13.89	25.29	8.48
0.0393	33.46	1.10	13.49	27.89	7.98
0.0434	31.75	1.21	13.12	30.76	7.52
0.0478	30.23	1.34	12.79	33.93	7.24
0.0527	28.88	1.48	12.50	37.42	7.08
0.0582	27.64	1.63	12.30	41.27	6.97
0.0642	26.50	1.79	12.25	45.52	6.83
0.0708	25.50	1.98	12.37	50.21	6.61
0.0780	24.60	2.18	12.69	55.38	6.15
0.0861	23.78	2.41	13.17	61.08	5.76
0.0949	23.05	2.66	13.70	67.36	5.56
0.105	22.38	2.93	14.16	74.30	5.43
0.115	21.78	3.23	14.46	81.95	5.37
0.127	21.24	3.56	14.72	90.38	5.36
0.140	20.74	3.93	14.90	99.69	5.42
0.155	20.29	4.33	14.98	109.95	5.50
0.171	19.88				



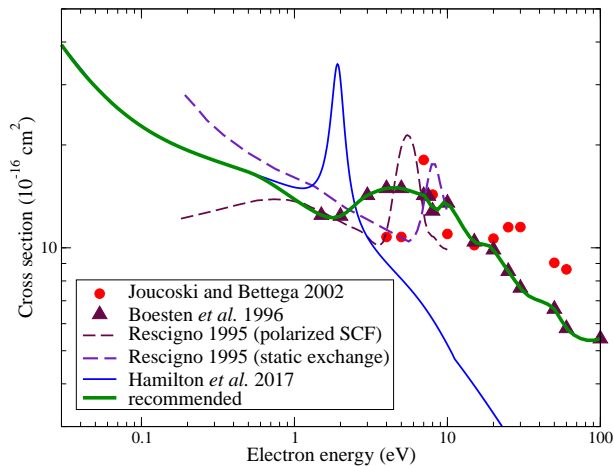


FIG. 5. The momentum-transfer cross section for elastic collisions obtained in different studies. The recommended data are shown by the thick green line. The data is the theoretical results by Hamilton *et al.*<sup>25</sup> below 0.65 eV and the experimental results by Boesten *et al.*<sup>15</sup> above 1.5 eV.

the rotational angular momentum  $j$  and its projection  $k$  on the molecular symmetry axis. The fluorine atom has only one stable isotope,  $^{19}\text{F}$  with nuclear spin  $i = 1/2$ . Therefore, the total nuclear spin of three fluorine atoms could be  $I = 1/2$  (para- $\text{NF}_3$ ) or  $3/2$  (ortho- $\text{NF}_3$ ). In the following discussion, we neglect the hyper-fine interaction and mixing between singlet and triplet nuclear-spin states of  $\text{NF}_3$ . The total wave function, including the nuclear-spin part, of  $\text{NF}_3$  should be of the  $A_2$  irreducible representation of the  $C_{3v}$  group because  $^{19}\text{F}$  is a fermion. It means that for ortho- $\text{NF}_3$ , the space part (rovibronic) of the wave function should also be of the  $A_2$  irreducible representation, because the nuclear spin part is totally symmetric,  $A_1$ . For para- $\text{NF}_3$ , the space part of the wave function should be of the  $E$  irreducible representation. In the both cases, it leads to the conclusion that the lowest allowed rotational level in the ground *vibronic* state has  $j = 1$ . The  $j = 0$  rotational level is forbidden for the ground *vibronic* state because the  $j = 0$  rotational level is of the  $A_1$  representation. For certain excited vibrational or/and electronic states of  $E$  and  $A_2$  representations of the  $\nu_3$  and  $\nu_4$  modes, the  $j = 0$  rotational level is allowed.

The only published data on rotational excitation is a theoretical calculation by Goswami *et al.*<sup>24</sup>, where rotational excitation cross sections starting from  $j = 0$  were calculated using the UK R-matrix code and the Quantemol interface<sup>36</sup>. In order to account for transitions starting from a  $j = 1$  rotational ground state, we employed a similar procedure using the scattering wave functions of Hamilton *et al.*<sup>25</sup> and, in the outer region, the experimental value for the  $\text{NF}_3$  dipole moment. Our new data are reproduced in Fig. 6 and numerical values are given in Table V. The magnitudes of the  $\Delta j = 0$  transition cross sections presented here are similar those calculated by Goswami *et al.*<sup>24</sup>. The main differences arise in region of the two shape resonances. The location of the resonances

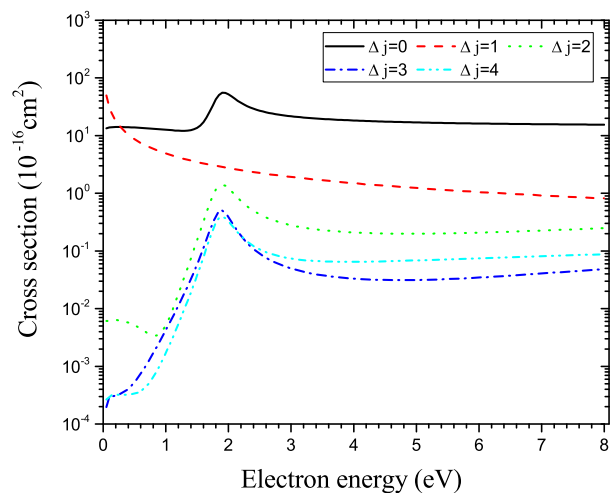


FIG. 6. Rotational excitation cross section from the ground rotational level  $j = 1$  to the  $j' = 1 - 5$  levels.

features in Fig. 6 are in agreement with a measured values of Nandi *et al.*<sup>20</sup> at 1.855 – 1.914 eV; the resonances of Goswami *et al.* are placed higher, at around 4 eV. The dipole-allowed,  $\Delta j = 1$  cross sections calculated in this work are larger than those of Goswami *et al.* This is due the different initial  $j$ , and subsequent  $j'$ , states considered. Our  $\Delta J > 1$  transition cross sections are of similar magnitude to those calculated by Goswami *et al.*, except when they are affected by the location of the shape resonances.

We also performed a quick calculation to estimate the uncertainty of the obtained cross sections due to parameters of the quantum-chemistry model used. The estimated uncertainty is about 5% for elastic  $\Delta j = 0$  transition, and about 20% for inelastic transitions.

## VI. VIBRATIONAL EXCITATION CROSS SECTIONS

The  $\text{NF}_3$  molecule has four vibrational modes, two of which are  $A_1$  non-degenerate modes,  $\nu_1$  and  $\nu_2$ , and the two others,  $\nu_3$  and  $\nu_4$ , are doubly-degenerate of  $E$  symmetry<sup>15</sup>. The excitation energies of the modes are given in Table VI.

The only available experimental data on vibrational excitation is by Boesten *et al.*<sup>15</sup> where differential cross sections for excitation of the  $\nu_1/\nu_3$  modes were measured in a crossed-beam experiment. The cross sections obtained are reproduced in Fig. 7. Figure 8 shows the cross section integrated over the solid angle. The corresponding numerical values are given in Table VII. Because the differential cross section was not measured for angles below  $20^\circ$  and above  $130^\circ$ , performing the integration, we assumed that the DCS below  $20^\circ$  is equal to the one at  $20^\circ$  and the DCS above  $130^\circ$  is equal to the one at  $130^\circ$ . Such an assumption introduces a significant uncertainty, of the order of 30%, into the integrated cross section.

TABLE V. The recommended cross sections for rotational excitation from the ground rotational level  $j = 1$  to the  $j' = 1 - 5$  levels. Energies are in eV, the cross sections are in units of  $10^{-16} \text{ cm}^2$ .

Electron Energy	CS $\Delta j = 0$	CS $\Delta j = 1$	CS $\Delta j = 2$	CS $\Delta j = 3$	CS $\Delta j = 4$
0.05	13.41	49.59	6.115E-03	1.960E-04	2.643E-04
0.10	13.85	30.61	6.176E-03	3.019E-04	3.130E-04
0.15	14.01	22.61	6.293E-03	3.038E-04	3.169E-04
0.20	14.07	18.11	6.325E-03	3.113E-04	3.192E-04
0.25	14.08	15.20	6.275E-03	3.239E-04	3.202E-04
0.30	14.06	13.15	6.155E-03	3.428E-04	3.206E-04
0.35	14.02	11.62	5.974E-03	3.700E-04	3.213E-04
0.40	13.97	10.44	5.740E-03	4.080E-04	3.231E-04
0.45	13.90	9.48	5.462E-03	4.599E-04	3.274E-04
0.50	13.82	8.70	5.149E-03	5.298E-04	3.357E-04
0.55	13.74	8.05	4.813E-03	6.224E-04	3.502E-04
0.60	13.64	7.49	4.467E-03	7.439E-04	3.735E-04
0.65	13.53	7.01	4.128E-03	9.016E-04	4.094E-04
0.70	13.42	6.60	3.820E-03	1.105E-03	4.625E-04
0.75	13.30	6.23	3.572E-03	1.366E-03	5.394E-04
0.80	13.18	5.90	3.422E-03	1.699E-03	6.484E-04
0.85	13.05	5.61	3.423E-03	2.125E-03	8.009E-04
0.90	12.92	5.35	3.642E-03	2.667E-03	1.012E-03
0.95	12.78	5.11	4.173E-03	3.358E-03	1.303E-03
1.00	12.64	4.90	5.142E-03	4.242E-03	1.701E-03
1.05	12.51	4.70	6.719E-03	5.374E-03	2.244E-03
1.10	12.38	4.52	9.142E-03	6.832E-03	2.986E-03
1.15	12.26	4.35	1.274E-02	8.718E-03	4.002E-03
1.20	12.16	4.20	1.799E-02	1.118E-02	5.395E-03
1.25	12.10	4.06	2.554E-02	1.441E-02	7.317E-03
1.30	12.10	3.93	3.637E-02	1.871E-02	9.987E-03
1.40	12.40	3.69	7.420E-02	3.237E-02	1.902E-02
1.50	13.63	3.48	1.533E-01	5.857E-02	3.763E-02
1.60	17.12	3.29	3.218E-01	1.120E-01	7.771E-02
1.70	25.92	3.13	6.627E-01	2.232E-01	1.637E-01
1.80	42.51	2.99	1.160E+00	4.090E-01	3.081E-01
1.85	50.83	2.93	1.343E+00	4.859E-01	3.701E-01
1.90	55.37	2.87	1.404E+00	5.021E-01	3.911E-01
1.95	55.23	2.80	1.349E+00	4.579E-01	3.697E-01
2.00	52.04	2.74	1.226E+00	3.873E-01	3.266E-01
2.05	47.80	2.68	1.083E+00	3.185E-01	2.808E-01
2.10	43.65	2.62	9.487E-01	2.617E-01	2.408E-01
2.20	37.01	2.51	7.369E-01	1.836E-01	1.824E-01
2.30	32.45	2.42	5.942E-01	1.372E-01	1.458E-01
2.40	29.30	2.33	4.978E-01	1.084E-01	1.223E-01
2.50	27.06	2.25	4.306E-01	8.935E-02	1.065E-01
2.60	25.40	2.17	3.822E-01	7.618E-02	9.543E-02
2.70	24.13	2.10	3.461E-01	6.666E-02	8.750E-02
2.80	23.12	2.04	3.185E-01	5.955E-02	8.166E-02
2.90	22.31	1.98	2.969E-01	5.409E-02	7.728E-02
3.00	21.64	1.92	2.796E-01	4.981E-02	7.396E-02
3.50	19.49	1.68	2.302E-01	3.789E-02	6.611E-02
4.00	18.29	1.50	2.095E-01	3.314E-02	6.490E-02
4.50	17.50	1.35	2.010E-01	3.140E-02	6.623E-02
5.00	16.93	1.23	1.993E-01	3.136E-02	6.863E-02
5.50	16.52	1.13	2.020E-01	3.250E-02	7.150E-02
6.00	16.20	1.05	2.079E-01	3.454E-02	7.456E-02
6.50	15.97	0.98	2.161E-01	3.731E-02	7.774E-02
7.00	15.78	0.92	2.260E-01	4.065E-02	8.102E-02
7.50	15.62	0.87	2.369E-01	4.447E-02	8.443E-02
8.00	15.47	0.82	2.484E-01	4.867E-02	8.799E-02

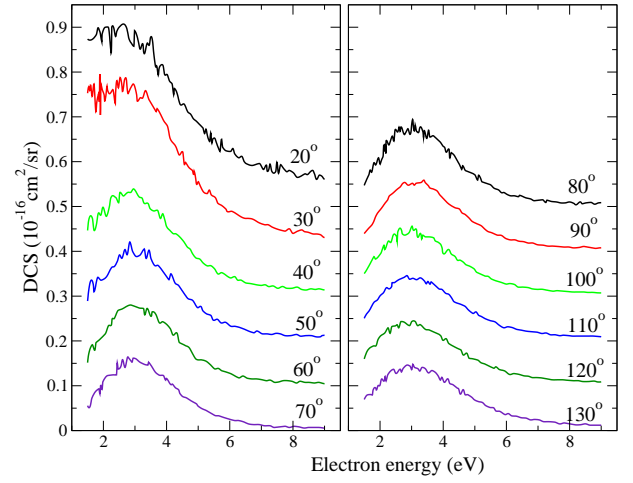


FIG. 7. Experimental differential cross section for excitation of the  $\nu_1/\nu_3$  modes<sup>15</sup>. The values for  $60^\circ$ ,  $70^\circ$ , etc. are shifted by 0.1, 0.2, etc. units and approach zero at 9 eV.

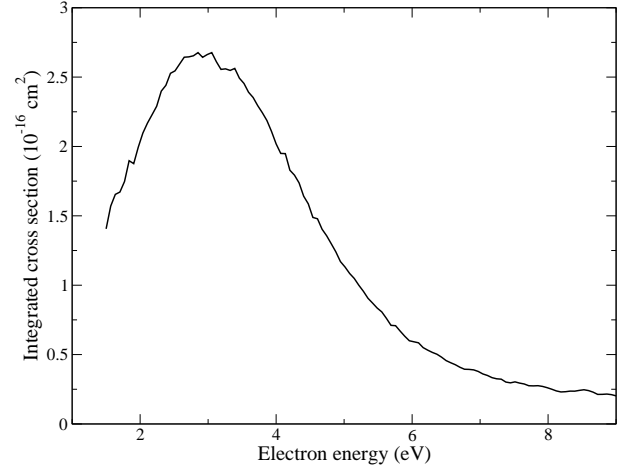


FIG. 8. Integrated cross section for excitation of the  $\nu_1/\nu_3$  modes obtained from the data shown in Fig. 7<sup>15</sup>.

Note that the present estimate of the vibrational cross section at 2.5 eV maximum agrees with the value used by Lisovskiy *et al.*<sup>26</sup> for modeling electron transport coefficients in NF<sub>3</sub>.

TABLE VI. Vibrational modes and excitation energies of NF<sub>3</sub><sup>15</sup>.

Mode	Type	Energy (eV)
$\nu_1$	Symmetric stretch	0.1280
$\nu_2$	Umbrella mode	0.0802
$\nu_3$	Asymmetric stretch	0.1125
$\nu_4$	Asymmetric bend	0.0611

TABLE VII. Integrated cross section for vibrational excitation of the  $\nu_1/\nu_3$  modes<sup>15</sup>. Electron energies are in eV, the cross sections are in units of  $10^{-16} \text{ cm}^{-1}$ .

Electron Energy	CS	Electron Energy	CS	Electron Energy	CS
1.50	1.41	4.07	1.95	6.57	0.44
1.57	1.57	4.14	1.95	6.64	0.43
1.64	1.65	4.20	1.83	6.70	0.41
1.70	1.67	4.27	1.79	6.77	0.39
1.77	1.75	4.34	1.74	6.84	0.39
1.84	1.90	4.41	1.64	6.91	0.39
1.91	1.88	4.47	1.59	6.97	0.38
1.97	1.99	4.54	1.49	7.04	0.36
2.04	2.10	4.61	1.48	7.11	0.35
2.11	2.17	4.68	1.40	7.18	0.33
2.18	2.23	4.74	1.36	7.24	0.33
2.24	2.29	4.81	1.30	7.31	0.32
2.31	2.40	4.88	1.24	7.38	0.30
2.38	2.44	4.95	1.17	7.45	0.30
2.45	2.53	5.01	1.13	7.51	0.30
2.51	2.54	5.08	1.08	7.58	0.29
2.58	2.59	5.15	1.05	7.65	0.29
2.65	2.64	5.22	1.00	7.72	0.28
2.72	2.65	5.28	0.96	7.78	0.27
2.78	2.65	5.35	0.91	7.85	0.28
2.85	2.68	5.42	0.87	7.92	0.27
2.92	2.64	5.49	0.84	7.99	0.26
2.99	2.66	5.55	0.81	8.05	0.25
3.05	2.68	5.62	0.76	8.12	0.24
3.12	2.61	5.69	0.71	8.19	0.23
3.19	2.56	5.76	0.71	8.26	0.23
3.26	2.56	5.82	0.67	8.32	0.24
3.32	2.55	5.89	0.63	8.39	0.24
3.39	2.56	5.96	0.60	8.46	0.24
3.46	2.49	6.03	0.59	8.53	0.25
3.53	2.45	6.09	0.58	8.59	0.24
3.59	2.39	6.16	0.55	8.66	0.23
3.66	2.35	6.23	0.53	8.73	0.21
3.73	2.29	6.30	0.52	8.80	0.21
3.80	2.24	6.36	0.50	8.86	0.22
3.86	2.19	6.43	0.48	8.93	0.21
3.93	2.11	6.50	0.46	9.00	0.20
4.00	2.02				

## VII. ELECTRON IMPACT ELECTRONIC EXCITATION AND DISSOCIATION

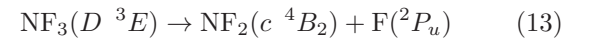
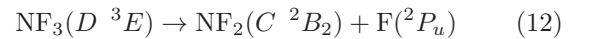
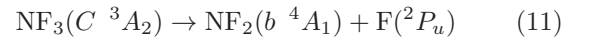
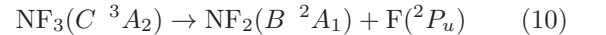
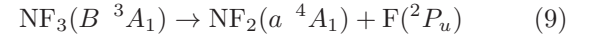
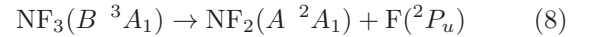
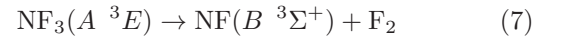
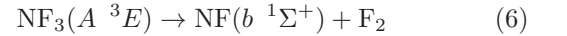
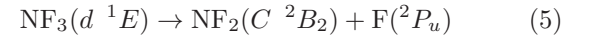
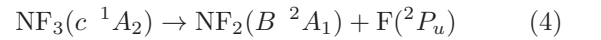
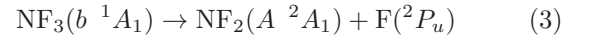
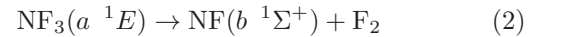
There are no experimental determinations of electron impact electronic excitation or dissociation. Theoretically Goswami *et al*<sup>24</sup> considered inelastic processes in their spherical complex optical potential (SCOP) calculations but this procedure does not separate these into their individual contributions. Here we therefore concentrate on the recent R-matrix calculation<sup>37</sup> by Hamilton *et al*<sup>25</sup> and older Kohn calculations by Rescigno<sup>22</sup>. Both calculations are based on the use of a close-coupling expansion of the target wave functions.

Electron impact dissociation reactions go via excitation to electronically excited states of the target which then dissociate<sup>38</sup>. The dissociation of the N-F in NF<sub>3</sub> is

2.52 eV<sup>39,40</sup> and no low-lying metastable electronically-excited states of NF<sub>3</sub> are known. It can therefore be assumed that all electronic excitation leads to dissociation; a similar assumption has been made in cases where the results are testable against experiment<sup>41</sup> and has been found to be reasonable. Both Rescigno and Hamilton *et al* made this assumption for NF<sub>3</sub>.

For an accurate calculation of these processes a large number of electronically excited states need to be considered. Born corrections to the electron-impact excitation cross sections were used to account for long range dipole effects<sup>42,43</sup>.

Hamilton *et al*<sup>25</sup> estimated the products of the dissociation process by analogy with the observed photodissociation cross sections of Seecombe *et al*.<sup>44</sup> which suggested that the following process can occur:



These results, which are given in Figure 9 and Table VIII, are the best currently available but they must be considered to be estimates. Experimental studies of electron impact dissociation of NF<sub>3</sub> would be very useful.

TABLE VIII. Cross sections for electron impact dissociation calculated by Hamilton *et al.*<sup>25</sup>; the products of the dissociation process were estimated by analogy with the observed photodissociation cross sections of Seccombe *et al.*<sup>44</sup>

Energy (eV)	Neutral Dissociation ( $10^{-16} \text{ cm}^2$ )	NF + F <sub>2</sub> ( $10^{-16} \text{ cm}^2$ )	NF <sub>2</sub> + F ( $10^{-16} \text{ cm}^2$ )	Energy (eV)	Neutral Dissociation ( $10^{-16} \text{ cm}^2$ )	NF + F <sub>2</sub> ( $10^{-16} \text{ cm}^2$ )	NF <sub>2</sub> + F ( $10^{-16} \text{ cm}^2$ )
8.63	0.04487	0.04487		10.91	0.25451	0.18656	0.05096
8.74	0.11003	0.11003		10.95	0.25555	0.18735	0.05115
8.86	0.13913	0.14		10.99	0.25605	0.18763	0.05131
8.97	0.15767	0.16		11.01	0.2562	0.18769	0.05138
9.09	0.17047	0.17		11.05	0.25636	0.18768	0.05151
9.20	0.17963	0.18		11.09	0.2564	0.18758	0.05161
9.32	0.18627	0.19		11.11	0.25638	0.18751	0.05166
9.43	0.19111	0.19		11.15	0.2563	0.18732	0.05173
9.54	0.19459	0.19		11.19	0.25616	0.18711	0.05178
9.66	0.19707	0.20		11.21	0.25607	0.18701	0.0518
9.77	0.19884	0.20		11.25	0.25587	0.1868	0.05181
9.89	0.20012	0.20		11.27	0.25575	0.1867	0.05179
10.00	0.20125	0.20		11.29	0.2556	0.18663	0.05173
10.01	0.20136	0.20136		11.31	0.25913	0.18676	0.05332
10.05	0.20186	0.20186		11.35	0.26174	0.18636	0.05495
10.09	0.20252	0.20252		11.39	0.26303	0.18612	0.05575
10.11	0.20296	0.20296		11.41	0.26359	0.18602	0.0561
10.15	0.20439	0.20439		11.45	0.26463	0.18582	0.05675
10.17	0.20583	0.20583		11.49	0.26562	0.18566	0.05735
10.19	0.21064	0.21064		11.50	0.26587	0.18562	0.0575
10.21	0.24834	0.20752	0.03062	11.89	0.27628	0.18605	0.06249
10.23	0.25086	0.20595	0.03368	12.27	0.2898	0.19053	0.06671
10.25	0.25271	0.20493	0.03583	12.66	0.30896	0.19843	0.0735
10.29	0.25521	0.20332	0.03892	13.05	0.33706	0.21021	0.08497
10.31	0.25608	0.2026	0.04011	13.43	0.36743	0.22496	0.09535
10.35	0.25731	0.20125	0.04205	13.82	0.40073	0.24445	0.10366
10.39	0.25805	0.19994	0.04358	14.20	0.43873	0.26877	0.11144
10.41	0.25828	0.1993	0.04424	14.59	0.48114	0.29735	0.11912
10.45	0.25853	0.19803	0.04537	14.98	0.52912	0.32951	0.12768
10.49	0.25854	0.19678	0.04632	15.36	0.58334	0.36512	0.1378
10.51	0.25847	0.19615	0.04674	15.75	0.64031	0.40123	0.14951
10.55	0.25822	0.19491	0.04748	16.14	0.69457	0.43312	0.16253
10.59	0.25784	0.19368	0.04812	16.52	0.73877	0.45673	0.17508
10.61	0.25761	0.19307	0.0484	16.91	0.77005	0.46928	0.18698
10.65	0.25706	0.19185	0.04891	17.30	0.78505	0.47031	0.19654
10.69	0.25643	0.19063	0.04935	17.68	0.78314	0.46111	0.20238
10.71	0.25608	0.19002	0.04954	18.07	0.7663	0.44414	0.20396
10.75	0.25532	0.1888	0.04989	18.45	0.7386	0.42244	0.20168
10.79	0.25448	0.18755	0.0502	18.84	0.70516	0.39907	0.19665
10.81	0.25402	0.1869	0.05034	19.23	0.67113	0.37657	0.19045
10.85	0.25298	0.18554	0.05059	19.61	0.64066	0.35669	0.18459
10.87	0.25233	0.18473	0.0507	20.00	0.6166	0.34047	0.18021
10.89	0.25335	0.18555	0.05084				

## VIII. IONIZATION CROSS SECTION

NF<sub>3</sub> ionization was measured in several experiments and calculated in Binary Encounter Bethe (BEB) model developed by Kim and Rudd.<sup>45</sup> Generally, the agreement between experiments and the theory is rather poor: experimental data are lower than values calculated. Recommended values from the Landolt-Börnstein review<sup>46</sup> were obtained as averages of Tarnovsky *et al.*<sup>47</sup> and Haaland *et al.*<sup>17</sup>. Total and partial ionization (into NF<sub>3</sub><sup>+</sup>, NF<sub>2</sub><sup>+</sup>, NF<sup>+</sup>, N<sup>+</sup>, NF<sub>3</sub><sup>2+</sup>, NF<sub>2</sub><sup>2+</sup>, NF<sup>2+</sup>) cross sections were compiled between 14-200 eV. No data was reported of

F<sup>+</sup> due to a serious disagreement between the two experiments. (Note that the figure in L-B is mislabeled). In Fig. 10 we compare the recommended values from L-B review that resumed earlier experiments, with the recent measurements of Rahman *et al.*<sup>18</sup>

Tarnovsky *et al.*<sup>16</sup> measured total and partial cross sections in two laboratories (using a magnetic selector and a fast-beam method). The agreement for the NF<sub>3</sub><sup>+</sup> parent ionization from the two laboratories is within 8%. Partial cross sections for NF<sub>2</sub><sup>+</sup>, NF<sup>+</sup>, F<sup>+</sup> ions were measured by the fast ion beam method. An upper limit for the formation of N<sup>+</sup> was also determined. Total declared



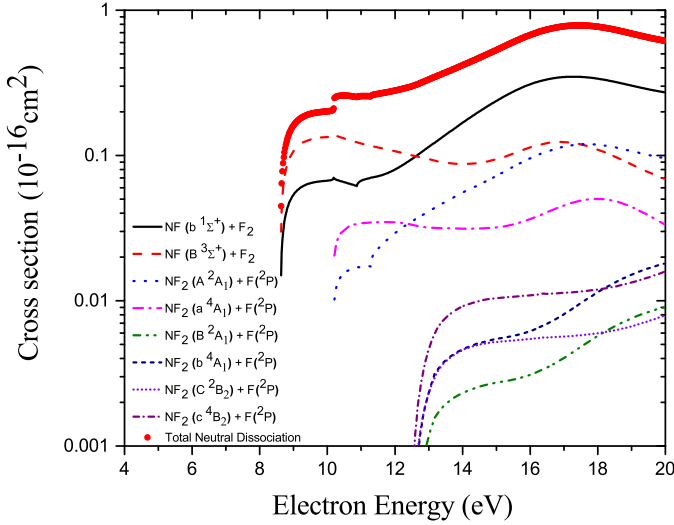


FIG. 9. Cross sections for electron impact dissociation into various channels, taken from the recent R-matrix calculation by Hamilton *et al.*<sup>25</sup>

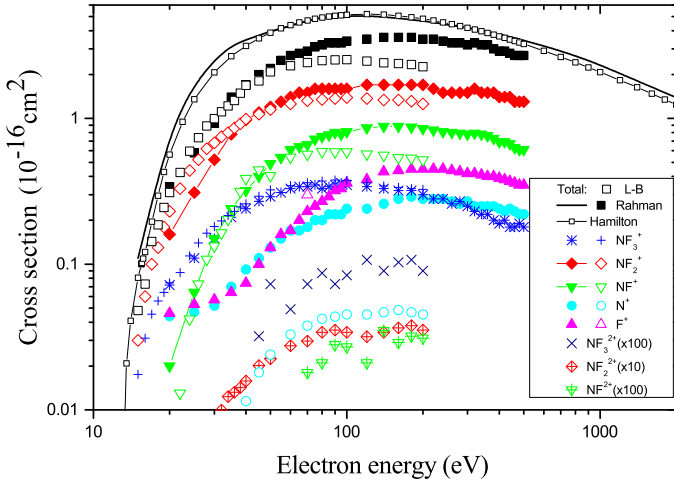


FIG. 10. Comparison of the compilation<sup>46</sup> of earlier experiments with the recent measurements by Rahman *et al.*<sup>18</sup> Closed symbols (squares, stars, diamonds, inverted triangles, circles, triangles) are Rahman *et al.*'s data (for total ionization, and production of  $\text{NF}_3^+$ ,  $\text{NF}_2^+$ ,  $\text{NF}^+$ ,  $\text{N}^+$  and  $\text{F}^+$  ions, respectively). Open symbols for  $\text{NF}_3^+$ ,  $\text{NF}_2^+$ ,  $\text{NF}^+$  are from the Landolt-Börnstein compilation<sup>46</sup>; an open circle and an open triangle are upper limits for  $\text{N}^+$  and  $\text{F}^+$  production, respectively, from Tarnovsky *et al.*'s experiment<sup>16</sup>. Crossed symbols (x, circles, inverted triangles) are L-B recommended values for doubly charged ions ( $\text{NF}_3^{2+}$ ,  $\text{NF}_2^{2+}$ ,  $\text{NF}^{2+}$ , respectively) – the data are based on measurements by Haaland *et al.*<sup>17</sup> (note the multiplying factors in figure). Thick black line is the total ionization in the complex-potential optical model by Rahman *et al.*<sup>18</sup>, thin black line with squares is the total ionization in BEB model by Hamilton *et al.*<sup>25</sup>

uncertainties on cross sections were  $\pm 20\%$ .

Haaland *et al.*<sup>17</sup> used a modified Fourier-transform mass spectrometry: ions were confined radially by a high (2T) magnetic field and axially by an electrostatic (1-2 V) potential. In this method no ions are actually collected but, instead, their electromagnetic influence on the antenna is recorded. Cross sections were normalized to Ar ionization cross sections of Wetzel<sup>48</sup>; the uncertainty of this normalization is  $\pm 12\%$ <sup>17</sup> and the declared total uncertainty  $\pm 16\%$ . Data for all partial processes, including double ionizations ( $\text{NF}_3^{2+}$ ,  $\text{NF}_2^{2+}$ ,  $\text{NF}^{2+}$ ) were reported up to 200 eV.

Rahman *et al.*<sup>18</sup> measured total and partial (but only for single ionization) cross sections up to 500 eV. They used a time-of-flight spectrometer with a 30 cm-long free-flight path for ions. They normalized relative data to the  $\text{Ar}^+$  ionization cross section at 100 eV of Krishnakumar and Srivastava<sup>49</sup>. Declared total uncertainty was  $\pm 15\%$ .

The best agreement (within some 15% up to 100 eV) between the three experiments<sup>16–18</sup> is seen for the  $\text{NF}_3^+$  parent ion; at higher energies data of Rahman *et al.*<sup>18</sup> and Tarnovsky *et al.*<sup>16</sup> still agree within 10% while results of Haaland *et al.* are somewhat (30% at 200 eV) higher. For  $\text{NF}_2^+$  the measurements of Rahman *et al.* agree very well (within 10%) with those by Haaland *et al.* but those of Tarnovsky *et al.* are by 30% lower at 200 eV. In turn, for  $\text{NF}^+$  ion the data of Haaland are somewhat lower (20% at 100 eV) than the two other sets considered here. Note from Fig. 10 that the experiment of Rahman *et al.*'s tends to produce higher cross sections for  $\text{NF}_2^+$  and  $\text{NF}^+$  ions than the recommended data from the Landolt-Börnstein<sup>46</sup> review; the same holds for the total ionization.

For light ions ( $\text{N}^+$  and  $\text{F}^+$ ) the results of Haaland *et al.*<sup>17</sup> are systematically lower (by a factor of about 10 for  $\text{F}^+$  and 50 for  $\text{N}^+$ ) than the data by Rahman *et al.*<sup>18</sup>. The upper limits for  $\text{N}^+$  and  $\text{F}^+$  at 100 eV given by Tarnovsky *et al.*<sup>16</sup> ( $0.1 \times 10^{-16}$  and  $0.3 \times 10^{-16}$  cm<sup>2</sup>, respectively) roughly agree with measurements by Rahman *et al.*, see Fig. 10. Some possible systematic errors are related to the experimental methods used. In Haaland *et al.*'s<sup>17</sup> experiment this is the indirect measurements of the signal from ions, clearly making uncertain the determination of partial cross sections for light ions like  $\text{N}^+$  and  $\text{F}^+$  (i.e. lighter than  $\text{Ar}^+$  used for normalization). On the other hand, this is the only experiment sufficiently sensitive to detect doubly charged molecular fragments,  $\text{NF}_3^{2+}$ ,  $\text{NF}_2^{2+}$ , and  $\text{NF}^{2+}$  with cross sections of the order  $10^{-20}$  –  $10^{-19}$  cm<sup>2</sup>, see table IX.

Another question is the dependence of the experimental sensitivity on the collision energy. The ion optics performs some focusing and the efficiency of ion collection can depend on their post-collisional velocities. As it was discussed for a long time in  $\text{CF}_4$ , see<sup>50</sup>, the problem is particularly difficult when ions are formed with high velocities, and through different fragmentation channels. For  $\text{NF}_3$  Tarnovsky *et al.*<sup>16</sup> observed that  $\text{NF}_2^+$  ions are formed with little excess kinetic energy for impact energies near the threshold but  $\text{NF}^+$  ions appear with a

broad distribution of excess kinetic energy, ranging from zero to about 4 eV.

In time-of-flight method some metastable ions can decay before reaching detector. A rough evaluation of flight times for heavier ions give values in the microseconds range – long enough for some fragmentation to occur. This, tentatively, would explain lower values of the  $\text{NF}_2^+$  cross section up to about 40 eV in Rahman *et al.*'s experiment as compared to the Landolt-Börnstein values, see Fig.10. In turn, cross sections for  $\text{N}^+$  and  $\text{F}^+$  show some unusual enhancement in this energy region, what would indicate some in-flight decay of heavier ( $\text{NF}_2^+$ ,  $\text{NF}^+$ ) ions, see Fig.10.

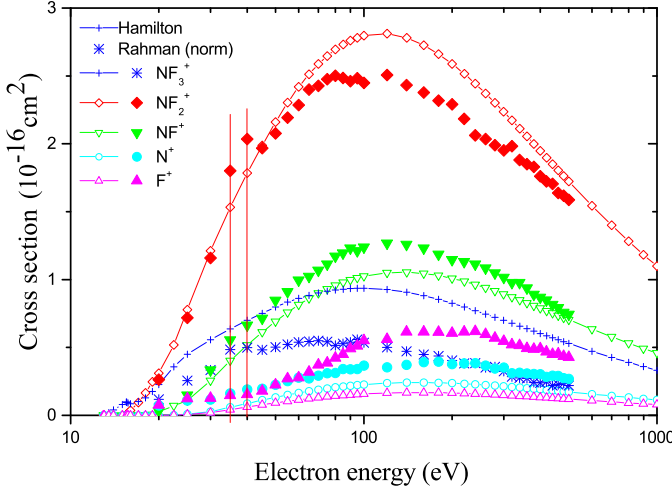


FIG. 11. Comparison of BEB-like partial cross sections by Hamilton *et al.*<sup>25</sup> with Rahman *et al.* measurements<sup>18</sup>. The latter partial cross sections (the sum of them) have been normalized, at each energy, to the BEB<sup>25</sup> total ionization cross section. Vertical lines (34.6 eV and 40.4 eV) show thresholds for ( $\text{F}^+ + \text{NF}^+ + \text{F}$ ) and ( $\text{F}^+ + \text{N}^+ + 2\text{F}$ ) channels.

### A. BEB model

The BEB model was employed by Huo *et al.*<sup>51</sup>, Haaland *et al.*<sup>17</sup> and Szmytkowski *et al.*<sup>14</sup> to calculate the ionization cross section of  $\text{NF}_3$  – all giving the maximum for the total ionization cross section of about  $4.8 \times 10^{-16} \text{ cm}^2$ . This agrees also with the “rule-of-thumb” noticed recently for the  $\text{CH}_4$ ,  $\text{CH}_3\text{F}$ , ...,  $\text{CF}_4$  series<sup>52</sup> that maximum in total ionization cross section (in  $10^{-16} \text{ cm}^2$ ) can be estimated as  $4/3\alpha$ , where the dipole polarizability  $\alpha$  of the molecule is expressed in  $10^{30} \text{ m}^3$  units. Using for  $\text{NF}_3$  the dipole polarizability of  $3.62 \times 10^{-30} \text{ m}^3$  from Ref.<sup>29</sup> one gets a maximum of the total ionization cross section of  $4.84 \times 10^{-16} \text{ cm}^2$ . Recently, Hamilton *et al.*<sup>25</sup> calculated BEB ionization cross sections using Dunning’s augmented Gaussian-type orbitals (aug-cc-pVTZ GTO) and obtained a somewhat higher total cross section maximum ( $5.19 \times 10^{-16} \text{ cm}^2$ ). Subsequently, they applied

the same BEB-like analytical expression to derive partial ionization cross sections, adapting appropriate threshold energies. Relative amplitudes were deduced from NIST(National Institute of Standards and Technology)<sup>27</sup> electron-impact ionization mass spectrum at 100 eV. Results for the total cross section are shown in Fig. 10 and for partial cross sections in Fig. 11. We adopt also these cross sections as recommended values, see table. XI. We note also, that BEB total cross section agrees very well with the optical complex-potential calculation by Rahman *et al.*<sup>18</sup>, see Fig. 10.

Fig.11 compares BEB<sup>25</sup> partial cross sections with the normalized partial cross sections of Rahman *et al.*. To do this normalization, the sum of experimental partial cross sections at every energy have been normalized to the BEB value; subsequently at this energy all partial cross sections have been multiplied by the factor obtained. The normalization factors range from 2.3 at 25 eV to 1.22 at 500 eV.

This comparison allows one to distinguish difference between the expected partial cross sections and those actually measured in the time-of-flight experiment. The  $\text{NF}_2^+$  experimental signal in the energy range above 50 eV is systematically lower than the BEB model; the same holds for the  $\text{NF}_3^+$  ion which was measured (in all three<sup>16–18</sup> experiments) to be roughly half as abundant as the BEB<sup>25</sup> values (that were obtained, we recall, via NIST mass spectrum). Figure 11 visualizes that the deficits in the  $\text{NF}_3^+$  and  $\text{NF}_2^+$  experimental abundances are compensated by higher values of  $\text{F}^+$ ,  $\text{NF}^+$  and  $\text{N}^+$  signals. This once again indicates some complex mechanisms of the dissociative ionization.

TABLE IX. Ionization cross sections for formation of doubly charged ions, from Landolt-Börnstein review<sup>46</sup> (based on Haaland *et al.*<sup>17</sup>) data. Cross sections are in  $10^{-18} \text{ cm}^2$  units. The overall uncertainty is  $\pm 50\%$

Energy (eV)	$\text{NF}_3^{2+}$ ( $10^{-18} \text{ cm}^2$ )	$\text{NF}_2^{2+}$ ( $10^{-18} \text{ cm}^2$ )	$\text{NF}^{2+}$ ( $10^{-18} \text{ cm}^2$ )
30	-	0.0589	-
32	-	0.0998	-
34	-	0.123	-
36	-	0.132	-
38	-	0.142	-
40	-	0.158	-
45	0.032	0.201	-
50	0.073	0.224	-
60	0.049	0.276	0.000
70	0.073	0.296	0.018
80	0.087	0.341	0.021
90	0.073	0.353	0.028
100	0.084	0.341	0.027
120	0.107	0.318	0.021
140	0.090	0.341	0.035
160	0.103	0.366	0.029
180	0.107	0.379	0.032
200	0.090	0.353	0.031

TABLE X. Threshold energy values (in eV) for various fragments observed and their comparison with earlier measurements. Observed thresholds are shown against the estimated ones, wherever possible.

Ions	Channel	$\Delta H^\circ$	Rahman <i>et al.</i> <sup>18</sup>	Reese <i>et al.</i> <sup>53</sup>	Tarnovsky <i>et al.</i> <sup>16</sup>
NF <sub>3</sub> <sup>+</sup>	NF <sub>3</sub> → NF <sub>3</sub> <sup>+</sup>	13.5	13.5 ± 0.6	13.2 ± 0.2	13.6 ± 0.2
NF <sub>2</sub> <sup>+</sup>	NF <sub>3</sub> → NF <sub>2</sub> <sup>+</sup> + F	14.0	14.5 ± 0.6	14.2 ± 0.3	14.5 ± 0.4
	→ NF <sub>2</sub> <sup>+</sup> + F <sup>-</sup>	10.4	-	-	-
NF <sup>+</sup>	-	-	16 ± 0.6	-	-
	NF <sub>3</sub> → NF <sup>+</sup> + 2F	17.45	17.5 ± 0.7	17.9 ± 0.3	17.6 ± 0.4
	→ NF <sup>+</sup> + F <sub>2</sub> <sup>-</sup>	14.45	-	-	-
	→ NF <sup>+</sup> + F + F <sup>-</sup>	13.85	-	-	-
	→ NF <sup>+</sup> + F <sup>+</sup> + F	34.6	-	-	-
F <sup>+</sup>	-	-	20 ± 0.7	-	-
	NF <sub>3</sub> → F <sup>+</sup> + NF <sub>2</sub> <sup>-</sup>	18.8	19 ± 1	-	-
	→ NF + F <sup>+</sup> + F	22.0	-	-	-
	→ N + 2F + F <sup>+</sup>	25.85	25 ± 1	25 ± 1	-
	→ F <sup>+</sup> + NF <sup>+</sup> + F	34.6	33 ± 1	-	36
N <sup>+</sup>	→ F <sup>+</sup> + N <sup>+</sup> + 2F	40.4	-	-	-
	NF <sub>3</sub> → N <sup>+</sup> + 3F	23.0	22 ± 1	22.2 ± 0.2	-
	→ N <sup>+</sup> + F + F <sub>2</sub> <sup>-</sup>	20.0	-	-	-
	→ N <sup>+</sup> + F <sup>-</sup> + F <sub>2</sub>	19.4	-	-	-

TABLE XI. Recommended ionization cross sections for NF<sub>3</sub>: BEB values from ref.<sup>25</sup>, see text). Energies are in eV, cross sections are in 10<sup>-16</sup> cm<sup>2</sup> units. The overall uncertainty is ±10% for total cross sections and ±20% for partial ones.

Energy	N <sup>+</sup>	F <sup>+</sup>	NF <sup>+</sup>	NF <sub>2</sub> <sup>+</sup>	NF <sub>3</sub> <sup>+</sup>	Total	Energy	N <sup>+</sup>	F <sup>+</sup>	NF <sup>+</sup>	NF <sub>2</sub> <sup>+</sup>	NF <sub>3</sub> <sup>+</sup>	Total
14	-	-	-	-	0.04	0.04	200	0.24	0.16	1.01	2.59	0.83	4.83
15	-	-	-	-	0.08	0.08	220	0.23	0.16	0.99	2.52	0.80	4.69
16	-	-	-	0.04	0.09	0.12	240	0.23	0.16	0.96	2.44	0.77	4.56
17	-	-	-	0.10	0.10	0.20	260	0.22	0.16	0.94	2.37	0.75	4.44
18	-	-	-	0.17	0.13	0.30	280	0.22	0.15	0.92	2.30	0.72	4.31
19	-	-	0.01	0.25	0.18	0.43	300	0.21	0.15	0.89	2.24	0.70	4.19
20	-	-	0.03	0.31	0.23	0.56	320	0.21	0.15	0.87	2.17	0.68	4.08
25	0.01	0.01	0.11	0.78	0.45	1.35	340	0.21	0.14	0.85	2.11	0.66	3.96
30	0.03	0.02	0.26	1.21	0.56	2.07	360	0.20	0.14	0.83	2.06	0.64	3.86
35	0.06	0.04	0.40	1.53	0.64	2.67	380	0.20	0.14	0.81	2.00	0.62	3.76
40	0.09	0.06	0.52	1.79	0.70	3.15	400	0.19	0.13	0.79	1.95	0.60	3.66
45	0.11	0.08	0.61	1.99	0.75	3.54	420	0.19	0.13	0.77	1.90	0.59	3.57
50	0.13	0.09	0.69	2.16	0.80	3.88	440	0.18	0.13	0.75	1.85	0.57	3.48
55	0.15	0.1	0.76	2.30	0.83	4.15	460	0.18	0.12	0.74	1.81	0.56	3.40
60	0.17	0.11	0.81	2.42	0.86	4.38	480	0.18	0.12	0.72	1.76	0.54	3.32
65	0.18	0.12	0.86	2.51	0.88	4.56	500	0.17	0.12	0.70	1.72	0.53	3.25
70	0.19	0.13	0.90	2.59	0.90	4.71	600	0.16	0.11	0.64	1.54	0.47	2.92
75	0.20	0.14	0.93	2.65	0.91	4.83	700	0.14	0.10	0.58	1.40	0.43	2.65
80	0.21	0.14	0.96	2.69	0.92	4.93	800	0.13	0.09	0.53	1.28	0.39	2.43
85	0.21	0.15	0.98	2.73	0.93	5.00	900	0.12	0.09	0.49	1.18	0.36	2.24
90	0.22	0.15	1.00	2.76	0.93	5.06	1000	0.11	0.08	0.46	1.10	0.33	2.08
95	0.22	0.16	1.01	2.78	0.94	5.11	1200	0.10	0.07	0.40	0.96	0.29	1.83
100	0.23	0.16	1.03	2.80	0.94	5.14	1400	0.09	0.06	0.36	0.86	0.26	1.63
120	0.24	0.16	1.05	2.81	0.93	5.19	1600	0.08	0.06	0.33	0.78	0.23	1.48
140	0.24	0.17	1.05	2.78	0.91	5.15	1800	0.08	0.05	0.30	0.71	0.21	1.35
160	0.24	0.17	1.05	2.73	0.88	5.06	2000	0.07	0.05	0.28	0.66	0.20	1.25
180	0.24	0.17	1.03	2.66	0.85	4.95							

### B. Dissociative ionization channels

Ionization threshold were thoroughly reported by Rahman *et al.*<sup>18</sup> and Tarnovsky *et al.*<sup>16</sup>. The threshold for  $\text{NF}_3^+$  parent ion is  $13.6 \pm 0.2$  eV<sup>16</sup>. The  $\text{NF}_2^+$  ion shows, according to Rahman *et al.*, two onsets, closely spaced (14.5 and 16 eV); note that only one value ( $14.5 \pm 0.4$  eV<sup>16</sup>) was reported by other experiments. see table X. Three onsets were identified by Tarnovsky *et al.* for the  $\text{NF}^+$  ion: ( $\text{NF}^+ + 2\text{F}$ ) at 17.6 eV, ( $\text{F}^+ + \text{NF}^+ + \text{F}$ ) at 36.5 eV (reported by Rahman *et al.*<sup>18</sup> in the  $\text{F}^+$  production channel) and another, not identified, at 21.8 eV, see table 3. Rahman *et al.* reported a threshold of  $19 \pm 1$  eV for  $\text{F}^+$  production and assigned it to the  $\text{NF}_3 \rightarrow \text{F}^+ + \text{NF}_2^-$  process. Note that this is the only reporting on the dipolar dissociation in  $\text{NF}_3$ .

### C. Recommended values

Taking into account the significant differences between experiments (and their different sensitivities), we decided to recommend total and partial ionization cross sections from the recent BEB analysis by Hamilton *et al.*<sup>25</sup>, detailed results of which are given in table XI. We stress that such a choice is not free of some coarse assumptions: the validity of BEB model for partial cross sections and correct procedures in measurements of partial ions in NIST experiment. We are also aware that our explanations for the differences between the most recent<sup>18</sup> and earlier experiments<sup>16,17</sup> are only tentative. Therefore, we refer the reader to data by Rahman *et al.*<sup>18</sup> (table 2 in their paper) as a complementary choice. In view of importance of  $\text{NF}_3$  for plasma processes in semiconductor industries, verification of cross section for total and partial ionization is urgent; new theories would be also welcome. The estimated uncertainty on presently recommended values is  $+10\% - 20\%$  for the total ionization and  $+20\% - 30\%$  for partial cross sections.

## IX. ELECTRON ATTACHMENT (DEA) CROSS SECTION

There are only two published reports, relevant to this evaluation purpose, on the absolute measurements of the dissociative electron attachment (DEA) cross sections for  $\text{NF}_3$ : Harland and Franklin<sup>19</sup> and Nandi *et al.*<sup>20</sup> Other than these, Chantry reported the DEA cross sections for  $\text{NF}_3$  at a conference and the results were also contained in a book<sup>21</sup> but were not published in a journal, and therefore, this will not be discussed any further here. There are two experimental determinations of the electron attachment coefficient in swarms,<sup>54,55</sup> but the two results are not consistent with each other and it is unclear which is more reliable. Harland and Franklin<sup>19</sup> employed a linear TOF mass spectrometer to measure translational energies of negative ions formed by dissociative resonance

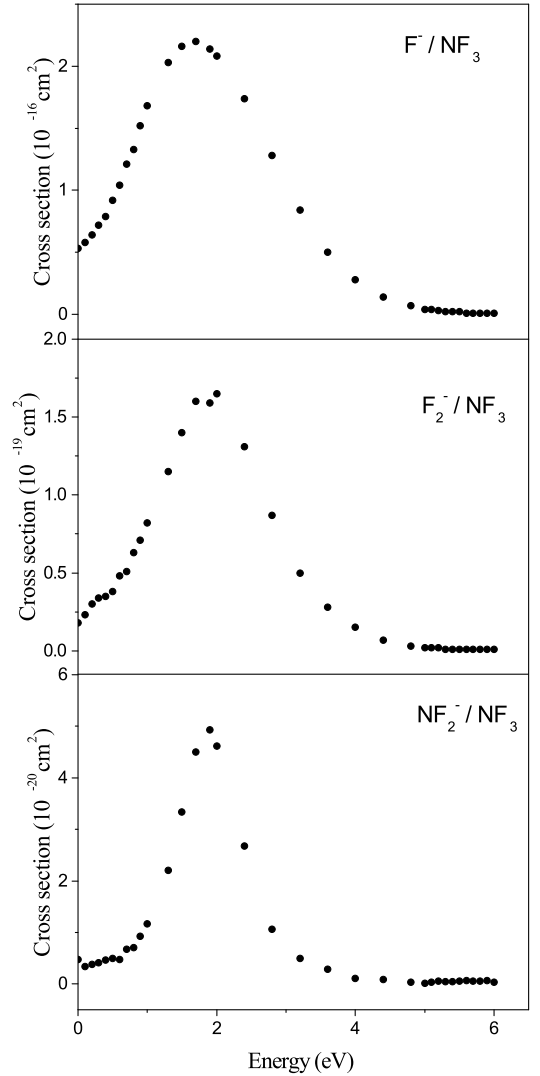


FIG. 12. . Recommended cross sections for the formation of  $\text{F}^-$ ,  $\text{F}_2^-$  and  $\text{NF}_2^-$  from  $\text{NF}_3$ . Note the different scales in cross sections<sup>20</sup>.

capture processes from  $\text{NF}_3$ . Nandi *et al.*<sup>20</sup> have pointed out that mass to charge ratio analysis becomes imperative for the measurement of partial cross sections when more than one type of ions are produced and then it is necessary that the extraction, mass analysis, and the detection procedures for these ions are carried out without discriminating against their initial kinetic energies, angular distributions or their mass to charge ratios. These necessitated them to use a crossed beam geometry and an efficient solution to these problems was to use a segmented time-of-flight (TOF) mass spectrometer along with the pulsed-electron-beam and pulsed-ion-extraction techniques and the relative flow technique. The results of Harland and Franklin<sup>19</sup> and Nandi *et al.*<sup>20</sup> agree well with each other in the positions of the resonance peaks, but the magnitude show the differences as nearly big as a factor of four. For example, the cross sections of the

formation of  $F^-$  are  $0.6 \times 10^{-16} \text{ cm}^2$  for Harland and Franklin and  $2.2 \times 10^{-16} \text{ cm}^2$  for Nandi *et al.* In both experiments,  $F^-$  is the most dominant ion from the DEA process with very small intensities of  $F_2^-$  and  $NF_2^-$ . For  $F_2^-$ , the cross section of Nandi *et al.* is smaller than that obtained by and Franklin. For  $NF_2^-$ , the cross section of Nandi *et al.* is larger than the corresponding data of Harland and Franklin within a factor of 2. For all the ions, there is a finite cross section even at zero energy. The electron beam has a halfwidth of 0.5 eV. It is possible that the high energy tail of the electron energy distribution is giving rise to the finite cross section at zero energy for  $F_2^-$  and  $NF_2^-$ <sup>20</sup>. The high resolution measurements of Ruckhaberle *et al.*<sup>56</sup> showed finite cross section for  $F^-$  at zero energy, whereas both  $F_2^-$  and  $NF_2^-$  appear only above 1 eV<sup>20</sup>. Considering the fact that Nandi *et al.* have made more complete measurements of the experimental parameters, we recommend their cross sections for the dissociative electron attachment process of  $NF_3$ . Complete numerical values of the recommended cross sections are presented in Table XII and Fig. 12. Nandi *et al.* estimated the uncertainty to be about 15%.

## X. SUMMARY AND FUTURE WORK

We present a systematic review of the published cross sections for processes resulting from electron collisions with  $NF_3$  up to the end of 2016. Both measurements and theoretical predictions are considered, although priority is given to high quality measurements with published uncertainties where available. The summary of cross section for electron collisions with  $NF_3$  is given in Fig. 13. There is considerable variation in the reliability of the available data. For the total cross section, the momentum transfer cross section and the ionization cross section, it is possible to recommend values over an extended energy range with small uncertainties, typically 10 to 15%. The situation is significantly worse for other processes. For electron impact rotational excitation we rely on predictions from *ab initio* calculations, but these calculations are far from being complete. The experimental work on this process would be welcome. There is one direct experimental measurements of electron impact vibrational excitation cross sections. Theoretical treatments of this process is possible and should be performed by theorists. Some new, reliable beam measurements of this process would be very helpful. Electron impact dissociation is an important process but the available measurements are inconsistent with each other and we are unable to recommend a good set of data for this process. A new study on the problem is needed. Finally there are two data available for the dissociative electron attachment process. Here we recommend using the most recent experimental data and are able to provide estimated uncertainty to be about 15%.

This evaluation is one in series of systematic evaluations<sup>33,57</sup> of electron collision processes for key

TABLE XII. Recommended dissociative attachment cross sections for the formation of  $F^-$ ,  $F_2^-$  and  $NF_2^-$  from  $NF_3$ <sup>20</sup>. The uncertainties are estimated to be about 15 %.

Energy (eV)	$\sigma(F^-)$ ( $10^{-16} \text{ cm}^2$ )	$\sigma(F_2^-)$ ( $10^{-19} \text{ cm}^2$ )	$\sigma(NF_2^-)$ ( $10^{-20} \text{ cm}^2$ )
0.0	0.53	0.18	0.48
0.1	0.58	0.23	0.34
0.2	0.64	0.30	0.38
0.3	0.72	0.34	0.41
0.4	0.79	0.35	0.46
0.5	0.92	0.38	0.50
0.6	1.04	0.48	0.47
0.7	1.21	0.51	0.67
0.8	1.33	0.63	0.71
0.9	1.52	0.71	0.93
1.0	1.68	0.82	1.17
1.3	2.03	1.15	2.20
1.5	2.16	1.40	3.34
1.7	2.20	1.60	4.50
1.9	2.14	1.59	4.93
2.0	2.08	1.65	4.62
2.4	1.74	1.31	2.68
2.8	1.28	0.87	1.06
3.2	0.84	0.50	0.50
3.6	0.50	0.28	0.29
4.0	0.28	0.15	0.11
4.4	0.14	0.07	0.09
4.8	0.07	0.03	0.03
5.0	0.04	0.02	0.01
5.1	0.04	0.02	0.03
5.2	0.03	0.02	0.06
5.3	0.02	0.01	0.05
5.4	0.02	0.01	0.05
5.5	0.02	0.01	0.06
5.6	0.01	0.01	0.07
5.7	0.01	0.01	0.06
5.8	0.01	0.01	0.06
5.9	0.01	0.01	0.07
6.0	0.01	0.01	0.03

molecular targets. Other evaluations will appear in future papers.

## XI. ACKNOWLEDGMENTS

This work was partially supported by the National Research Council of Science & Technology (NST) grant by the Korea government (MSIP) (No. PCS-17-05-NFRI). H. C. acknowledges the support from Chungnam National University in 2016. VK acknowledges partial support from the National Science Foundation, Grant No PHY-15-06391. GK acknowledges partial support from Grant 2014/15/D/ST2/02358 of National Science Center in Poland.



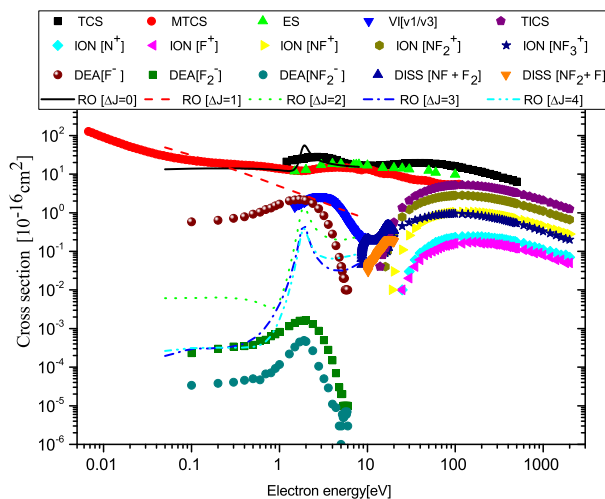


FIG. 13. The summary of cross section for electron collisions with  $\text{NF}_3$ . TCS - total scattering, ES - elastic scattering, MT - momentum transfer, ION - partial ionization, TICS - total ionization, VI - vibrational excitation, RO - rotational excitation, DEA - dissociative electron attachment, DISS - Neutral dissociation cross section

## XII. REFERENCES

- <sup>1</sup>S. Huang, V. Volynets, J. R. Hamilton, S. Lee, I.-C. Song, S. Lu, J. Tennyson, and M. J. Kushner, "Insights to scaling remote plasma sources sustained in  $\text{NF}_3$  mixtures," *J. Vac. Sci. Technol.* **35**, 031302 (2017).
- <sup>2</sup>L. Pruette, S. Karecki, R. Chatterjee, R. Reif, T. Sparks, and V. Vartanian, "High density plasma oxide etching using nitrogen trifluoride and acetylene," *J. Vac. Sci. Tech. A* **18**, 2749–2758 (2000).
- <sup>3</sup>J. M. Veilleux, M. S. El-Genk, E. P. Chamberlin, C. Munson, and J. FitzPatrick, "Etching of  $\text{UO}_2$  in  $\text{NF}_3$  RF plasma glow discharge," *J. Nuc. Mat.* **277**, 315–324 (2000).
- <sup>4</sup>G. Bruno, P. Capezzuto, G. Cicala, and P. Manodoro, "Study of the  $\text{NF}_3$  plasma cleaning of reactors for amorphous-silicon deposition," *J. Vac. Sci. Tech. A* **12**, 690–698 (1994).
- <sup>5</sup>B. E. E. Kastenmeier, P. J. Matsuo, G. S. Oehrlein, and J. G. Langan, "Remote plasma etching of silicon nitride and silicon dioxide using  $\text{NF}_3/\text{O}_2$  gas mixtures," *J. Vac. Sci. Technol. A* **16**, 2047–2056 (1998).
- <sup>6</sup>F. H. C. Goh, S. M. Tan, K. Ng, H. A. Naseem, W. D. Brown, and A. M. Hermann, "Fluorinated silicon-nitride (a-Si-N,F,H) films using  $\text{NF}_3$  for amorphous-silicon based solar-cells," in *Amorphous silicon technology - 1990*, Materials research society symposium proceedings, Vol. 192, edited by Taylor, P C and Thompson, M J and Lecomber, P G and Hamakaura, Y and Madan, A (MRS, Pittsburgh, PA, 1990) pp. 75–80.
- <sup>7</sup>S. Kurtz, R. Reedy, B. Keyes, G. Barber, J. Geisz, D. Friedman, W. McMahon, and J. Olson, "Evaluation of  $\text{NF}_3$  versus dimethylhydrazine as N sources for GaAsN," *J. Crystal Growth* **234**, 323–326 (2002).
- <sup>8</sup>J. B. Park, J. S. Oh, E. Gil, S.-J. Kyoung, J.-S. Kim, and G. Y. Yeom, "Plasma texturing of multicrystalline silicon for solar cell using remote-type pin-to-plate dielectric barrier discharge," *J. Phys. D: Appl. Phys.* **42**, 215201 (2009).
- <sup>9</sup>J. Gao, H. Zhu, Y. Wang, Z. Wang, F. Guan, J. Ni, J. Yin, L. Lan, Y. Bai, Y. Ma, Y. Mai, M. Wan, and Y. Huang, "Improvement of a-Si:H solar cell performance by  $\text{SiH}_4$  purging treatment," *Vacuum* **89**, 7–11 (2013).
- <sup>10</sup>M. C. Lin, "Chemical HF lasers from  $\text{NF}_3\text{-H}_2$  and  $\text{NF}_3\text{-C}_2\text{H}_6$  systems," *J. Chem. Phys.* **75**, 284–286 (1971).
- <sup>11</sup>A. M. Razhev, D. S. Churkin, E. S. Kargapol'tsev, and S. V. Demchuk, "Pulsed inductive HF laser," *Quant. Electron.* **46**, 210–212 (2016).
- <sup>12</sup>N. Posseme, V. Ah-Leung, O. Pollet, C. Arvet, and M. Garcia-Barros, "Thin layer etching of silicon nitride: A comprehensive study of selective removal using  $\text{NH}_3/\text{NF}_3$  remote plasma," *J. Vac. Sci. Technol.* **34**, 061301 (2016).
- <sup>13</sup>K.-C. Yang, S.-W. Park, and G.-Y. Yeom, "Low Global Warming Potential Alternative Gases for Plasma Chamber Cleaning," *Sci. Adv. Materials* **8**, 2253–2259 (2016).
- <sup>14</sup>C. Szymkowski, A. Domaracka, P. Mozejko, E. Ptasińska-Denga, L. Klosowski, M. Piotrowicz, and G. Kasperski, "Electron collisions with nitrogen trifluoride  $\text{NF}_3$  molecules," *Phys. Rev. A* **70**, 032707 (2004).
- <sup>15</sup>L. Boesten, Y. Tachibana, Y. Nakano, T. Shinohara, H. Tanaka, and M. Dillon, "Vibrationally inelastic and elastic cross sections for  $e^-$ - $\text{NF}_3$  collisions," *J. Phys. B: At., Mol. Opt. Phys.* **29**, 5475–5492 (1996).
- <sup>16</sup>V. Tarnovsky, A. Levin, K. Becker, R. Basner, and M. Schmidt, "Electron impact ionization of the  $\text{NF}_3$  molecule," *Int. J. Mass Spectrom.* **133**, 175–185 (1994).
- <sup>17</sup>P. D. Haaland, C. Q. Jiao, and A. Garscadden, "Ionization of  $\text{NF}_3$  by electron impact," *Chem. Phys. Lett.* **340**, 479 (2001).
- <sup>18</sup>M. Rahman, S. Gangopadhyay, C. Limbachiya, K. Joshipura, and E. Krishnakumar, "Electron ionization of  $\text{NF}_3$ ," *Int. J. Mass Spectrom.* **319**, 48–54 (2012).
- <sup>19</sup>P. W. Harland and J. L. Franklin, "Partitioning of excess energy in dissociative resonance capture processes," *J. Chem. Phys.* **61**, 1621–1636 (1974).
- <sup>20</sup>D. Nandi, S. A. Rangwala, S. V. K. Kumar, and E. Krishnakumar, "Absolute cross sections for dissociative electron attachment to  $\text{NF}_3$ ," *Int. J. Mass Spectro.* **205**, 111–117 (2001).
- <sup>21</sup>P. Chantry, "Dissociative attachment cross-section measurements in  $\text{F}_2$  and  $\text{NF}_3$ ," in *Bull. Am. Phys. Soc.*, Vol. 24 (1979) pp. 134–134.
- <sup>22</sup>T. N. Rescigno, "Low-energy electron collision processes in  $\text{NF}_3$ ," *Phys. Rev. A* **52**, 329–333 (1995).
- <sup>23</sup>E. Joucoski and M. H. F. Bettge, "Elastic scattering of low-energy electrons by  $\text{NF}_3$ ," *J. Phys. B: At., Mol. Opt. Phys.* **35**, 783–793 (2002).
- <sup>24</sup>B. Goswami, R. Nagma, and B. Antony, "Cross sections for electron collisions with  $\text{NF}_3$ ," *Phys. Rev. A* **88**, 032707 (2013).
- <sup>25</sup>J. R. Hamilton, J. Tennyson, S. Huang, and M. J. Kushner, "Calculated cross sections for electron collisions with  $\text{NF}_3$ ,  $\text{NF}_2$  and  $\text{NF}$ ," *Plasma Sources Sci. Technol.* **26**, 065010 (2017).
- <sup>26</sup>V. Lisovski, V. Yegorenkov, P. Ogloblina, J.-P. Booth, S. Martins, K. Landry, D. Douai, and V. Cassagne, "Electron transport parameters in  $\text{NF}_3$ ," *J. Phys. D: Appl. Phys.* **47**, 115203 (2014).
- <sup>27</sup>R. D. Johnson, "NIST computational chemistry comparison and benchmark d 17b, III (2015).
- <sup>28</sup>S. E. Novick, W. Chen, M. R. Munrow, and K. J. Grant, "Hyperfine structure in the microwave spectrum of  $\text{NF}_3$ ," *J. Mol. Spectrosc.* **179**, 219–222 (1996).
- <sup>29</sup>F. Macdonald and D. Lide, eds., *CRC Handbook of Chemistry and Physics* (CRC Press, Boca Raton, 2003-2004).
- <sup>30</sup>D. H. Shi, J. F. Sun, Z. L. Zhu, and Y. F. Liu, "Total cross sections of electron scattering by molecules  $\text{NF}_3$ ,  $\text{PF}_3$ ,  $\text{N}(\text{CH}_3)_3$ ,  $\text{P}(\text{CH}_3)_3$ ,  $\text{NH}(\text{CH}_3)_2$ ,  $\text{PH}(\text{CH}_3)_2$ ,  $\text{NH}_2\text{CH}_3$  and  $\text{PH}_2\text{CH}_3$  at 30–5000 eV," *Eur. Phys. J. D* **57**, 179–186 (2010).
- <sup>31</sup>G. Karwasz, T. Wróblewski, R. Brusa, and E. Illenberger, "Electron scattering on triatomic molecules: The need for data," *Japanese Journal of Applied Physics*, Japanese Journal of Applied Physics **45**, 8192 (2006).
- <sup>32</sup>M. H. F. Bettge, C. Winstead, V. McKoy, and C. I. o. T. A. A. Noyes Laboratory of Chemical Physics, "Low-energy electron scattering by  $\text{N}_2\text{O}$ ," *Phys. Rev. A* **74**, 022711 (2006).
- <sup>33</sup>M.-Y. Song, J.-S. Yoon, H. Cho, Y. Itikawa, G. P. Karwasz, V. Kokouline, Y. Nakamura, and J. Tennyson, "Cross sections

- for electron collisions with methane,” *J. Phys. Chem. Ref. Data* **44**, 023101 (2015).
- <sup>34</sup>A. Zecca, G. Karwasz, R. Brusa, and R. Grisenti, “Absolute total cross section measurements for intermediate-energy electron scattering. IV. Kr and Xe,” *Journal of Physics B: Atomic, Molecular and Optical Physics*, *J. Phys. B: At., Mol. Opt. Phys.* **24**, 2737 (1999).
- <sup>35</sup>A. Zecca, G. P. Karwasz, and R. S. Brusa, “Electron scattering by Ne, Ar and Kr at intermediate and high energies, 0.5–10 keV,” *J. Phys. B: At., Mol. Opt. Phys.* **33**, 843 (2000).
- <sup>36</sup>J. Tennyson, D. B. Brown, J. J. Munro, I. Rozum, H. N. Varambha, and N. Vinci, “Quantemol-N: an expert system for performing electron molecule collision calculations using the R-matrix method,” *J. Phys. Conf. Series* **86**, 012001 (2007).
- <sup>37</sup>J. M. Carr, P. G. Galiatsatos, J. D. Gorfinkiel, A. G. Harvey, M. A. Lysaght, D. Madden, Z. Masin, M. Plummer, and J. Tennyson, “The UKRmol: a low-energy electron- and positron-molecule scattering suite,” *Euro. Phys. J. D* **66**, 58 (2012).
- <sup>38</sup>D. T. Stibbe and J. Tennyson, “Near-threshold electron impact dissociation of H<sub>2</sub>,” *New J. Phys.* **1**, 2 (1998).
- <sup>39</sup>V. I. Vedeneyev, L. V. Gurvich, V. N. Kondrat’ev, V. A. Medvedev, and Y. L. Frankevich, “Chemical bond energies, ionization potentials and electron affinities,” (Edward Arnold, Ltd., London, 1966), translation of 1962 Russian edition (1962).
- <sup>40</sup>A. Kennedy and C. B. Colburn, “Strength of the N–F bonds in NF<sub>3</sub> and of N–F and N–N bonds in N<sub>2</sub>F<sub>4</sub>,” *J. Chem. Phys.* **35**, 1892–1893 (1961).
- <sup>41</sup>W. J. Brigg, J. Tennyson, and M. Plummer, “R-matrix calculations of low-energy electron collisions with methane,” *J. Phys. B: At. Mol. Opt. Phys.* **47**, 185203 (2014).
- <sup>42</sup>S.-I. Chu and A. Dalgarno, “Rotational excitation of CH<sup>+</sup> by electron impact,” *Phys. Rev. A* **10**, 788–792 (1974).
- <sup>43</sup>K. L. Baluja, N. J. Mason, L. A. Morgan, and J. Tennyson, “Electron scattering from ClO using the R-matrix method,” *J. Phys. B: At., Mol. Opt. Phys.* **33**, L677–L684 (2000).
- <sup>44</sup>D. P. Secombe, R. P. Tuckett, H.-W. Jochims, and H. Baumgärtel, “The observation of fluorescence from excited states of NF<sub>2</sub> and NF following the photodissociation of NF<sub>3</sub> in the 11–30 eV range,” *Chem. Phys. Lett.* **339**, 405–412 (2001).
- <sup>45</sup>Y.-K. Kim and M. E. Rudd, “Binary-encounter-dipole model for electron-impact ionization,” *Phys. Rev. A* **50**, 3954–3967 (1994).
- <sup>46</sup>M. T. Elford, *Photon and Electron Interactions with Atoms, Molecules, and Ions (Landolt-Börnstein: Numerical Data and Functional Relationships in Science and Technology / Elementary Particles, Nuclei and Atoms)*, edited by W. Martinussen, Vol. 17 (Springer, New York, 2003).
- <sup>47</sup>V. Tarnovsky, A. Levin, and K. Becker, “Absolute cross sections for the electron impact ionization of the NF<sub>2</sub> and NF free radicals,” *J. Chem. Phys.* **100**, 5626–5630 (1994).
- <sup>48</sup>R. C. Wetzel, F. A. Baiocchi, T. R. Hayes, and R. S. Freund, “Absolute cross sections for electron-impact ionization of the rare-gas atoms by the fast-neutral-beam method,” *Phys. Rev. A* **35**, 559–577 (1987).
- <sup>49</sup>E. Krishnakumar and S. K. Srivastava, “Ionisation cross sections of rare-gas atoms by electron impact,” *J. Phys. B: At., Mol. Opt. Phys.* **21**, 1055–1082 (1988).
- <sup>50</sup>M. R. Bruce and R. A. Bonham, “On the partial ionization cross-sections for CF<sub>4</sub> by use of the pulsed-electron-beam time-of-flight method,” *Int. J. Mass Spectr.* **123**, 97–100 (1993).
- <sup>51</sup>W. M. Huo, V. Tarnovsky, and K. H. Becker, “Total electron-impact ionization cross-sections of CF<sub>x</sub> and NF<sub>x</sub> (x= 1–3),” *Chem. Phys. Lett.* **358**, 328–336 (2002).
- <sup>52</sup>G. P. Karwasz, P. Mozejko, and M.-Y. Song, “Electron-impact ionization of fluoromethanes—review of experiments and binary-encounter models,” *Int. J. Mass Spectr.* **365**, 232–237 (2014).
- <sup>53</sup>R. M. Reese and V. H. Dibeler, “Ionization and dissociation of nitrogen trifluoride by electron impact,” *J. Chem. Phys.* **24**, 1175–1177 (1956).
- <sup>54</sup>K. Nygaard, H. Brooks, and S. Hunter, “Negative ion production rates in rare gas-halide lasers,” *IEEE J. Quant. Electron.* **15**, 1216–1223 (1979).
- <sup>55</sup>V. K. Lakdawala and J. L. Moruzzi, “Measurements of attachment coefficients in NF<sub>3</sub>-nitrogen and NF<sub>3</sub>-rare gas mixtures using swarm techniques,” *J. Phys. D: Appl. Phys.* **13**, 377–386 (1980).
- <sup>56</sup>N. Ruckhaberle, L. Lehmann, S. Matejcek, E. Illenberger, Y. Bouteiller, V. Periquet, L. Museur, C. Desfrancois, and J.-P. Schermann, “Free electron attachment and rydberg electron transfer to NF<sub>3</sub> molecules and clusters,” *J. Phys. Chem. A* **101**, 9942–9947 (1997).
- <sup>57</sup>M.-Y. Song, J.-S. Yoon, H. Cho, Y. Itikawa, G. P. Karwasz, V. Kokoouline, Y. Nakamura, and J. Tennyson, “Cross sections for electron collisions with acetylene,” *J. Phys. Chem. Ref. Data* **46**, 013106 (2017).

